



Altered *PTPRD* DNA methylation associates with restricted adipogenesis in healthy first-degree relatives of Type 2 diabetes subjects

Luca Parrillo^{‡,1}, Rosa Spinelli^{‡,1}, Michele Longo^{‡,1}, Antonella Desiderio¹, Paola Mirra¹, Cecilia Nigro¹, Francesca Fiory¹, Shahram Hedjazifar², Margherita Mutarelli³, Annamaria Carissimo³, Pietro Formisano¹, Claudia Miele¹, Ulf Smith², Gregory Alexander Raciti¹ & Francesco Beguinot^{*,1}

¹URT Genomics of Diabetes-IEOS, CNR & Department of Translational Medicine – Federico II University of Naples, 80131, Italy

²Lundberg Laboratory for Diabetes Research, Department of Molecular & Clinical Medicine, Sahlgrenska Academy, University of Gothenburg, Gothenburg, 41345, Sweden

³Telethon Institute of Genetics & Medicine (TIGEM), Pozzuoli 80078, Italy

*Author for correspondence: Tel.: +39 081 746 3248; Fax: +39 081 746 3235; beguino@unina.it

[‡]Authors contributed equally

Aim: First-degree relatives (FDR) of individuals with Type 2 diabetes (T2D) feature restricted adipogenesis, which render them more vulnerable to T2D. Epigenetics may contribute to these abnormalities. **Methods:** FDR pre-adipocyte *Methylome* and Transcriptome were investigated by MeDIP- and RNA-Seq, respectively. **Results:** *Methylome* analysis revealed 2841 differentially methylated regions (DMR) in FDR. Most DMR localized into gene-body and were hypomethylated. The strongest hypomethylation signal was identified in an intronic-DMR at the *PTPRD* gene. *PTPRD* hypomethylation in FDR was confirmed by bisulphite sequencing and was responsible for its upregulation. Interestingly, *Ptprd*-overexpression in 3T3-L1 pre-adipocytes inhibited adipogenesis. Notably, the validated *PTPRD*-associated DMR was significantly hypomethylated in peripheral blood leukocytes from the same FDR individuals. Finally, *PTPRD* methylation pattern was also replicated in obese individuals. **Conclusion:** Our findings indicated a previously unrecognized role of *PTPRD* in restraining adipogenesis. This abnormality may contribute to increase FDR proclivity toward T2D.

First draft submitted: 12 September 2019; Accepted for publication: 17 March 2020; Published online: 2 June 2020

Keywords: adipose tissue • DNA methylation • epigenetics • gene expression • pre-adipocyte • Type 2 diabetes

Subcutaneous adipose tissue (SAT) has been identified as a key player in the evolution toward Type 2 diabetes (T2D) [1]. Limited SAT expandability induces hypertrophy and alters the secretion profile in mature adipose cells, causes low-grade chronic inflammation, ectopic fat accumulation and peripheral insulin resistance [2]. In humans, SAT hypertrophy results from an attenuated differentiation capacity of resident pre-adipocytes rather than lack of precursor cells [3]. Importantly, the increased adipose cell size predicts T2D even independent of obesity [4].

First-degree relatives of Type 2 diabetics (FDR) have up to tenfold increased risk of developing diabetes [5]. Healthy FDR also feature dysfunctional SAT and show signs of inflammation and macrophage infiltration accompanied by adipocyte hypertrophy, due to the impaired commitment and/or differentiation of SAT-resident pre-adipocytes [3,4,6]. These findings indicated that, in FDR, diabetes risk is associated to reduced ability to recruit new adipocytes in response to stimuli promoting adipose tissue expansion, inducing ectopic accumulation of fat, insulin resistance and rendering these individuals more vulnerable to T2D development.

The molecular mechanisms responsible for the restricted adipogenesis in FDR remain unclear. Despite intensive efforts to identify risk loci contributing to limited adipose tissue expandability [7], no genotype accounting for this defect in most FDR individuals has been so far identified. Environmental cues, which are also shared within the family groups, may attenuate the individual adipogenic potential leading to resident fat cell hypertrophy [8–10].

Accumulating evidence now identifies the epigenome as a signal integrator active at the interface between the environment and the function of genes whose alterations impact on evolution toward T2D [11]. Indeed, epigenetic changes may convert environmental cues into phenotypic traits by reprogramming transcription and contributing to disease development and/or transmission [12]. In addition, recent human studies in both SAT specimen [13,14] and SAT-derived pre-adipocytes [15,16], have revealed the important role of DNA methylation in the functional regulation of genes determining adipogenesis [2,13–17]. Thus, the hypothesis that epigenetic dysregulation impacts on FDR risk of T2D by impairing adipogenesis in the SAT deserves to be mechanistically investigated. There is presently no information on *Methylome* profile diversities in adipocyte precursor cells from healthy individuals who are FDR and subjects with no family history of T2D.

In the present work, we report the first genome-wide DNA methylation profile in adipocyte precursor cells from the SAT stromal vascular fraction (SVF) of healthy FDR and matched individuals with no T2D familiarity. These studies have established that, in FDR individuals, the excess risk of T2D is associated with hypomethylation events affecting major molecular pathways involved in transduction of signals controlling adipogenesis. Our data revealed a previously undescribed role of *PTPRD* in regulating adipogenesis.

Materials & methods

Study participants

Discovery cohort

Individuals with one ascertained first-degree relative with T2D ($n = 9$; FDR) and 11 subjects with no family history of T2D (control [CTRL]) were selected from the European Network on Functional Genomics of Type 2 Diabetes (EUGENE2) consortium [18]. The recruitment and clinical phenotyping of the subjects have been previously described [18]. The participants included in this study were healthy nondiabetic offspring of parents with T2D. For inclusion, one of the parents had to have T2D and the other parent normal glucose tolerance evaluated by an oral glucose tolerance test (OGTT) or lack of any family history of T2D. The study was approved by the appropriate institutional review board.

Abdominal SAT biopsies were obtained by needle aspiration from the paraumbilical region. Following careful dissection, adipose tissue specimens were digested with collagenase for 45 min at 37°C. After digestion, the suspension was centrifuged in two phases: an upper (fat cells) and a lower (SVF cells) phase. The isolated fat cells were filtered through a 250 μm nylon mesh, washed four-times with fresh medium for removal of collagenase. Cell size of isolated adipocytes was measured as described in [19]. The isolated SVF cells were washed twice and the erythrocytes were lysed with 155 mmol/l NH_4Cl for 5 min before seeding SVF in a 55- cm^2 petri dish. After 3 days, the inflammatory cells ($\text{CD}14^+$ and $\text{CD}45^+$ cells) and endothelial cells ($\text{CD}31^+$ cells) were removed from the adipocyte precursor cell fraction by immune magnetic separation (Miltenyi Biotech, Bergisch Gladbach, Germany). The adipocyte precursor cells were then cultured with DMEM:F12 medium (LONZA, Basel, Switzerland) supplemented with 10% fetal bovine serum (ThermoFisher Scientific, MA, USA), 2 mmol/l glutamine, 100 U/ml penicillin and 100 $\mu\text{g}/\text{ml}$ streptomycin (LONZA). After 2 weeks, any remaining inflammatory cells were removed by immune magnetic separation as described in [4,19].

Replication cohort

20 caucasian individuals from an independent cohort recruited at the Federico II University of Naples were included in the replication analysis. The cohort included ten obese patients and ten lean individuals (Supplementary Table 1). Recruitment and clinical phenotyping of these subjects have been previously described [20]. The study was approved by the Ethics Committee of the Federico II University of Naples (Ethics Approval Number: No. 254/17) and all subjects provided written informed consent for sampling.

MeDIP-Seq

Genomic DNA (gDNA), obtained from isolated SVF cells, was extracted using the AllPrep DNA/RNA Universal Kit (Qiagen, Hilden, Germany) according to the manufacturer's protocol. All gDNA samples were tested for integrity and quantified by using a Qubit 4 Fluorometer (ThermoFisher Scientific). Equimolar amounts of gDNA for each subject were pooled (two pools for each condition). Methylated DNA Immunoprecipitation followed by massively parallel sequencing (MeDIP-Seq) was performed by Beijing Genomics Institute (<https://www.bgi.com/global/>). Sequencing was performed on a HiSeq 2000 system (Illumina Inc., CA, USA). Reads were mapped to the reference human genome (hg19 release) using SOAP2.21 aligner (<http://soap.genomics.org.cn>). Read alignments

in sequence alignment map format were converted to binary alignment map for further analyses using SAMtools [21] and browser extensible data (BED)tools were used to convert mapped reads in BED format and to generate Bedgraph files uploaded in UCSC Genome Browser (<http://genome.ucsc.edu>). MeDIP-Seq datasets obtained were independently analyzed for whole genome peak scanning by MACS2 (<http://liulab.dfci.harvard.edu/MACS/>) [22]. By using BEDtools, we defined a set of common peaks within each experimental condition (both in CTRL and FDR individuals). $\geq 50\%$ overlap across the entire peak length was used as arbitrary threshold for the inclusion in this common set of peaks. The genomic coordinates of these peaks were extracted and unique reads mapping within these regions were used to compute differential methylation between CTRL and FDR individuals. Then, differentially methylated regions (DMR) in the comparison FDR versus CTRL subjects were computed using the R/Bioconductor package edgeR [23] and Benjamini–Hochberg approach was used for multiple testing correction [24]. For further analyses, only regions with an arbitrary threshold of 5% false discovery rate (fdr) were selected. The relative position of the peaks and proximity to genes were assessed using the online tool PAVIS2 [24]. The functional annotation tool DAVID (<https://david.ncifcrf.gov/home.jsp>) was used to classify genes with methylation peaks according to their biological function. Also see Supplementary methods for details.

RNA-Seq

Total RNA, obtained from isolated SVF cells, was extracted using the AllPrep DNA/RNA Universal Kit. RNA samples were tested for integrity and quantified by using a Qubit 4 Fluorometer. Equimolar amounts of total RNA for each subject were pooled (two pools for each condition). RNA-Seq was carried out by Beijing Genomics Institute (<https://www.bgi.com/global/>). Trimmed reads were aligned to Gencode Human release v19 transcripts by running RSEM version 1.2.19 with standard parameters [25]. Aligned reads (about 47 million per sample) were then used to estimate the expression level of each Gencode gene. Only genes with at least one count per million reads (CPM) in at least two samples were considered as expressed. Differential expression analysis between CTRL and FDR individuals was performed on the read counts of the expressed genes. The Generalized Linear Model approach implemented in the R/Bioconductor package edgeR was used to correct for possible bias [23]. The Benjamini–Hochberg approach was used for multiple testing correction [24]. Genes with \log_2 Fold Change (\log_2 FC) ≥ 1 and an $\text{fdr} \leq 0.05$ were considered as differentially expressed genes (DEG). To assess the robustness of our pooling design, we performed further RNA-Seq analyses on individual samples of total RNA from SAT pre-adipocytes of FDR and CTRL subjects. Also see Supplementary Methods for details.

Bisulphite sequencing

Bisulphite treatment of gDNA extracted from SVF and peripheral blood leukocytes (PBL) by the AllPrep DNA/RNA Mini Kit (Qiagen, Hilden, Germany), was performed using the EZ DNA Methylation Kit (Zymo Research, CA, USA). Converted gDNA was amplified by PCR using specific primers for *PTPRD*-DMR. Bisulphite sequencing (BS) was performed as reported in [17]. Primers are shown in Supplementary Table 2. See Supplementary Methods for details.

Total RNA isolation & quantitative real-time PCR

Total RNA was extracted from SVF and 3T3-L1 cells using the AllPrep DNA/RNA Mini Kit (Qiagen). Real-time RT-PCR was performed as described in [26]. Primers are shown in Supplementary Table 2. See Supplementary methods for details.

Western blots

Western blots were carried out as described in [26]. Immunoblots were performed with antibodies against DNMT3A (ab2850, Abcam, Cambridge, UK) and β -ACTIN (sc-47778, Santa Cruz Biotechnology, TX, USA).

Human SVF cell culture & treatment

SVF cells, isolated from control donors, at passages 3–5 were treated with 5-azacytidine (5'AZA; Sigma-Aldrich, MO, USA) for 2 days. See Supplementary methods for details.

Luciferase assay

The *PTPRD*-associated DMR *chr9:10448607-10450000* was amplified by PCR and cloned into a CpG-free promoter firefly luciferase reporter vector (pCpGL-promoter; InvivoGen, CA, USA). Luciferase assays were performed

Table 1. Clinical characteristics of first-degree relative and CTRL subjects.

Measure	FDR	CTRL
N (females/males)	9 (5/4)	11 (6/5)
Age, years	42.3 ± 2.9	38.7 ± 2.3
BMI, kg/m ²	25.4 ± 0.5	24.5 ± 0.7
Fat percent, %	26.9 ± 2.4	24.0 ± 1.9
Waist to hip ratio (WHR)	0.90 ± 0.02 [‡]	0.81 ± 0.02
Total triglycerides, mmol/l	1.5 ± 0.6 [‡]	0.8 ± 0.2
HDL cholesterol, mmol/l	1.3 ± 0.2 [†]	1.6 ± 0.3
Cell size, μ m	100.2 ± 1.7 [§]	89.4 ± 1.9
GIR/bw, mg/kg/min	7.9 ± 0.6 [‡]	11.5 ± 0.8
f-insulin, pmol/l	60.1 ± 8.0 [‡]	35.4 ± 3.9
fb-glucose, mmol/l	4.8 ± 0.1 [‡]	4.4 ± 0.1
OGTT p-glucose 2 h, mmol/l	6.6 ± 0.6 [†]	4.8 ± 0.4
HOMA-IR index	2.0 ± 0.8 [§]	1.1 ± 0.4

Clinical characteristics of FDR and CTRL subjects. All data are expressed as means ± SD. Statistical significance was tested by a two-tailed Mann–Whitney U-test.

[†]p < 0.05.

[‡]p < 0.01.

[§]p < 0.001, FDR vs CTRL.

BMI: Body mass index; CTRL: Control; f-insulin: Fasting insulin; fb-glucose: Fasting blood-glucose; FDR: First-degree relatives; GIR/bw: Glucose infusion rate/body weight; HDL: High-density lipoproteins; HOMA-IR: Homeostatic model assessment of insulin resistance; OGTT: Oral glucose tolerance test; p-glucose: Plasma-glucose.

as reported [27]. Constructs were transfected into ChubS7 pre-adipose cell line by lipofectamine (ThermoFisher Scientific), following manufacturer's instructions. Firefly luciferase activity was normalized against renilla luciferase activity (Promega, WI, USA). See Supplementary methods for details.

Overexpression of *Ptprd* in 3T3-L1 pre-adipocytes

3T3-L1 cells were grown and allowed to differentiate as described in [28,29]. Six hours before adipogenesis induction, 3T3-L1 pre-adipocytes were transfected with *Ptprd*-overexpressing vector (pCMV-*Ptprd*) or control vector (pCMV) using lipofectamine (ThermoFisher Scientific), following manufacturer's instructions. See Supplementary methods for details.

Statistical analysis

Data are expressed as mean ± SD. Mann–Whitney U-test was used to compare anthropometric and biochemical variables, gene expression and DNA methylation data between groups. The correlation between quantitative variables was tested using Spearman's rank correlation test. Two-tailed Student's t-test or the one-way analysis of variance (ANOVA) followed by Tukey's multi-comparison test was used, as appropriate, for the *in vitro* data. The group size (*n*) for each experimental group/condition is reported in the figure legends. The value of *n* refers to either the number of biological independent samples/individuals per group (*in vivo* analyses) or the number of independently repeated experiments, each performed at least in triplicate (*in vitro* studies). Differences were considered statistically significant at a p < 0.05. Statistical analyses were performed using the GraphPad Software (version 6.01, CA, USA).

Results

Differential DNA methylation in pre-adipocytes from first-degree relatives of individuals with T2D

To explore the molecular bases of the increased risk of T2D in FDR individuals, we have first selected a suitable study group from the EUGENE2 population [18]. As shown in Table 1, these subjects were healthy and nonobese individuals with (*n* = 9; FDR) or without (*n* = 11; CTRL) one first-degree relative with T2D and matched for age, BMI, body fat percentage and distribution. As described in [4], individuals who were FDR featured significantly reduced insulin sensitivity, increased HOMA-IR values, higher fasting plasma insulin and glucose levels and higher glucose levels following 75 g glucose loading. Also, the FDR had higher triglyceride levels and a reduced amount of high-density lipoproteins cholesterol compared with the CTRL individuals. Importantly, FDR also featured larger subcutaneous adipose cells when compared with control subjects, consistent with the finding that FDR individuals have subcutaneous adipose cell hypertrophy [4].

Table 2. DMR distribution in first-degree relative subjects.

Genomic features	Hypo-DMR in FDR	Hyper-DMR in FDR
Upstream	199	16
5'-UTR	25	-
Exon/CD	343	4
Intron	1955	188
3'-UTR	80	3
Downstream	26	2

DMR distribution in FDR subjects. The number and distribution of identified hypo- and hypermethylated DMR across different gene elements (e.g., 5'-UTR, Exons/CD, Intron, 3'-UTR) in the FDR samples.
 CD: Coding sequence; DMR: Differentially methylated region; FDR: First-degree relatives; UTR: Untranslated region.

We then hypothesized that increased risk of T2D in FDR is contributed by epigenetic changes impairing pre-adipocyte differentiation. To explore this possibility, we have used SVF adipocyte precursor cells from the abdominal SAT of the FDR and control individuals shown in Table 1. Genomic DNA from these individuals was subjected to MeDIP-Seq. We have generated about 180 million reads per sample, 70% of which could be uniquely aligned to the human genome. These reads were uniformly distributed through the entire SVF genome, as indicated by detection of methylation events in most chromosomal regions (data not shown). Subsequent analyses were exclusively based on these sequences.

To identify DMR associated with T2D family history, MeDIP-Seq profiles from the FDR and control individuals were compared. This analysis led us to identify 2841 unique DMR, 2628 of which were hypomethylated with further 213 resulting hypermethylated in FDR. The highest frequency of DMR was observed in the gene bodies, particularly in the intronic (2143) and the exonic (346) regions, where hypomethylation events were more common (Table 2).

DNA methyltransferases in FDR pre-adipocytes

We then sought to explore whether differences in the DNA methylation profile observed in the FDR subjects can be attributed to changes in the expression of DNA-methylating enzymes and therefore we focused our attention on the three catalytically active DNA methyltransferases (*DNMT3*) [17,30]. In SVF isolated from the FDR group, we observed a significant reduction in the mRNA expression of *DNMT3A*, which is responsible for *de novo* methylation events (Figure 1A). Furthermore, the amounts of DNMT3A protein in the SVF were decreased in the FDR compared with the control subjects (Figure 1B). No significant difference was found in the expression of *DNMT1* and *DNMT3B* between FDR and control subjects (Supplementary Figure 1), suggesting that the global hypomethylation observed in the SVF of the FDR individuals is contributed by reduced expression of DNMT3A. Interestingly, *DNMT3A* mRNA levels inversely correlated to the adipocyte cell size in the study group (Figure 1C).

DMR-associated genes feature functions related to adipocyte biology & T2D

Further analysis revealed that, in the FDR, 2392 genes overlapped the identified DMR with their promoter and/or gene body regions. These were termed differentially methylated genes (DMG), >90% of which featured decreased methylation signals. We then adopted the DAVID annotation tools (<http://david.ncifcrf.gov/home.jsp>) to analyze the identified DMG for over-representation of specific pathways. Interestingly, over-represented pathways were found to include the *Protein Kinase A*, *Insulin/IGF pathway-Protein Kinase B signalling*, *Inflammation by chemokine and cytokine pathway*, *Fibroblast Growth Factor signalling pathway* and the *WNT/ β -catenin signalling pathway*, all of which are linked to adipocyte cell function and T2D development (Supplementary Table 3).

Transcriptional effect of differential methylation

To explore the functional relevance of the FDR differential methylation, we complemented the *Methylome* dataset with *Transcriptome* analysis of SVF from FDR and control individuals. RNA-Seq analysis revealed 31 genes which were differentially expressed between FDR and control subjects. Out of these genes, 12 appeared to be downregulated while 19 were upregulated in FDR. We then merged the *Transcriptome* data with the identified intragenic DMR aiming at sorting differentially methylated sequences associated to functional effects on gene transcription. Three SVF genes exhibited significant expression changes associated to intragenic DMR in the FDR (Table 3). Interestingly, the expression-associated differential methylation changes occurred in gene body sequences

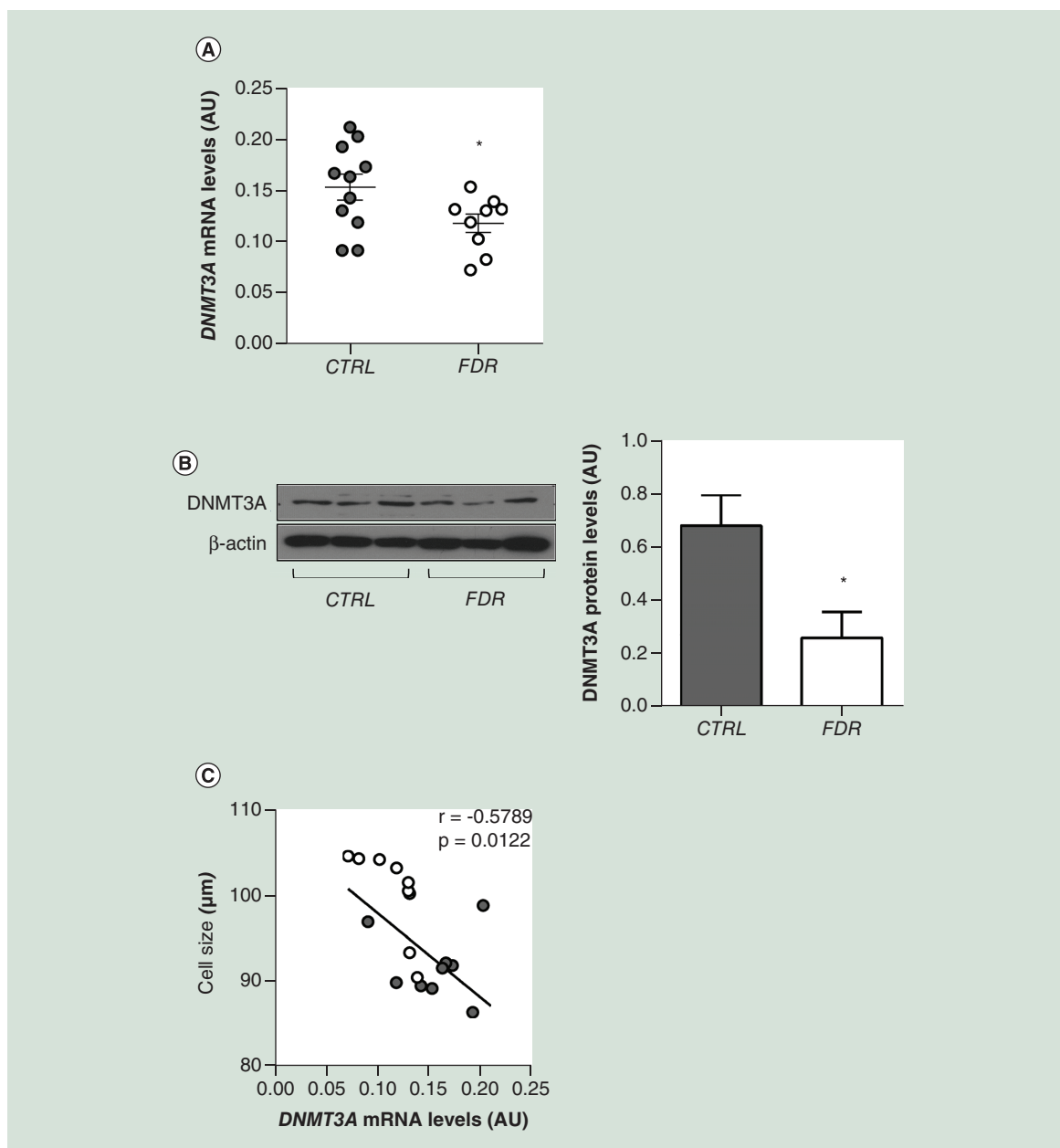


Figure 1. DNMT3A mRNA expression in subcutaneous pre-adipocytes from first-degree relative and CTRL subjects. (A) DNMT3A mRNA expression was measured by qPCR in SVF from FDR (n = 9) and control (CTRL; n = 11) subjects. Data points represent AU from each individual subject. Mean values \pm SD are also shown. * $p < 0.05$ in a two-tailed Mann–Whitney U-test. (B) Representative immunoblot analysis of DNMT3A and β -ACTIN protein levels in SVF from FDR (n = 6) and control (CTRL; n = 6) subjects. Data are expressed as arbitrary units and shown as mean values \pm SD. * $p < 0.05$ in a two-tailed Mann–Whitney U-test. (C) Correlation between SVF DNMT3A mRNA levels and adipose cell size in FDR (n = 9) and CTRL (n = 11) subjects. r correlation coefficient and p values are indicated on the graph. AU: Absolute units; CTRL: Control; FDR: First-degree relatives; SD: Standard deviation; SVF: Stromal vascular fraction cells.

rather than in promoter regions, underlining the significance of gene body methylation to transcriptional regulation.

To validate these findings, we focused on the *PTPRD* gene, previously associated to risk of T2D [31]. This gene was also found to be upregulated in FDR subjects by additional sequencing of individual samples from our study group (Supplementary Table 4). MeDIP-Seq analysis identified six hypomethylated DMR in *PTPRD* gene body spanning a region encompassing gene intron 1 to exon 12 (Table 4). DMR exhibiting the higher significance was

Table 3. List of the genes differentially methylated and expressed between first-degree relative and CTRL subjects.

Gene symbol	Gene name	log FC expression	log FC methylation	Relative location of DMR
<i>PTPRD</i>	Protein tyrosine phosphatase, receptor type D	1.43	-1.46	Inside intron [†]
<i>A2M</i>	Alpha-2-macroglobulin	1.13	-0.62	Intron/exon
<i>CADPS</i>	Ca ²⁺ -dependent secretion activator	1.71	-0.87	Inside intron

List of the genes differentially methylated and expressed between FDR and CTRL subjects. Genes exhibiting significant expression changes associated to intragenic DMR in the FDR. Differences in mRNA expression and DNA methylation are given as logarithmic fold change (*log FC*), consistently standardized in relation to CTRL subjects.

[†] *PTPRD*-associated DMR exhibiting the higher significance as described further on.

CTRL: Control; DMR: Differentially methylated region; FC: Fold change; FDR: First-degree relatives.

Table 4. Characteristics of hypomethylated DMR associated with *PTPRD* in first-degree relative subjects.

GENE	DMR number	Chromosome and position	Relation to gene region	Relation to CpG island	q-value
<i>PTPRD</i>	Medip_406	chr9:10448607-10450000	Intron	Yes	3.62E-07
	Medip_3624	chr9:9617306-9618320	Intron	No	1.57E-02
	Medip_4422	chr9:10018162-10019196	Intron	Yes	3.17E-02
	Medip_1540	chr9:10171213-10172126	Intron	No	5.30E-04
	Medip_3179	chr9:8712562-8714121	Intron	Yes	9.89E-03
	Medip_4937	chr9:9133607-9134817	Intron	Yes	4.43E-02

Characteristics of hypomethylated DMR associated with *PTPRD* in FDR subjects. Summary of *PTPRD*-associated DMR according to chromosome position, gene element and CpG context. *PTPRD*-DMR validated by bisulphite sequencing is in bold. P values have been adjusted for multiple testing using false discovery rate method.

Chr: Chromosome; DMR: Differentially methylated region; FDR: First-degree relatives.

subjected to bisulphite sequencing, which provided direct confirmation of DNA hypomethylation in the FDR (Figure 2A). Importantly, as shown in Figure 2B, *PTPRD* gene exhibited significant overexpression in the FDR compared with the control group that was inversely correlated to its hypomethylation (Figure 2C). Of note, *PTPRD* DNA methylation (Figure 3A) and its mRNA levels (Figure 3B) significantly correlated with adipose cell size in the same FDR and control individuals.

Functional analysis of *PTPRD* intronic DMR

To further explore the transcriptional consequence of the hypomethylation occurring at the *PTPRD* intronic DMR in FDR individuals, we exposed SVF cells to the demethylating agent 5-azacytidine (5'AZA). As shown in Supplementary Figure 2, we observed that, in parallel with reducing DNA methylation, 5'AZA treatment significantly upregulated *PTPRD* transcription.

To assess this issue mechanistically, we have used a CpG-free promoter plasmid with luciferase reporter gene (pCpGL) where the *PTPRD*-associated DMR *chr9:10448607-10450000* was cloned upstream the luciferase gene. This construct was then methylated *in vitro* or mock-treated and transfected in ChubS7 cells. In luciferase assays, the unmethylated *PTPRD*-associated DMR construct (pCpGL-*PTPRD* DMR) showed higher luciferase activity compared with the mock-treated empty vector (pCpGL; Figure 4). In contrast, the methylated *PTPRD*-associated DMR construct exhibited a significantly decreased transcriptional activity compared with the unmethylated pCpGL-*PTPRD* DMR (Figure 4), indicating that the intronic DMR functions as a DNA methylation-sensitive region regulating *PTPRD* expression.

Ptprd restrains adipogenic differentiation in 3T3-L1 pre-adipocytes

We have also examined whether *PTPRD* has a functional role in adipogenesis *in vitro*. To explore this possibility, 3T3-L1 pre-adipocytes were transfected with a pCMV vector expressing *Ptprd*. Eight days after the exposure to the differentiation cocktail, the cells overexpressing *Ptprd* accumulated significantly fewer lipids than either untransfected or empty vector transfected cells, as revealed by Oil Red O staining (Figure 5A & B). In parallel, expression of adipogenic markers was reduced in 3T3-L1 overexpressing *Ptprd* (Figure 5C-E), indicating that, *in vitro*, adipogenesis is impaired by *Ptprd* overexpression.

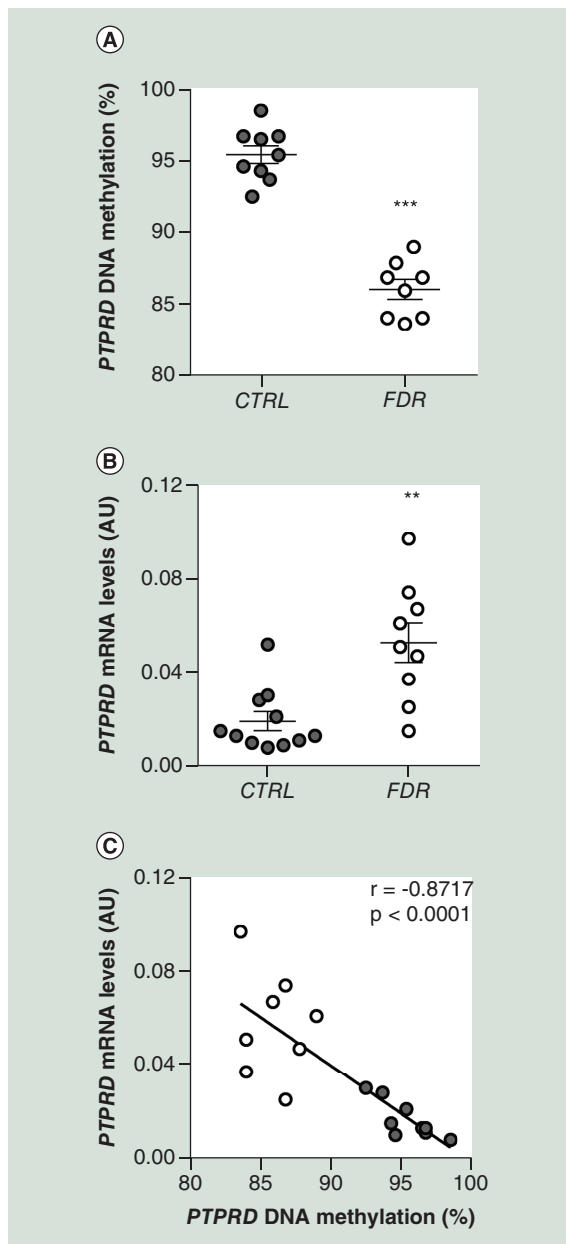


Figure 2. *PTPRD* DNA methylation and mRNA expression in subcutaneous pre-adipocytes from first-degree relative and CTRL subjects. (A) BS analysis of *PTPRD* DMR in SVF from FDR (n = 8) and CTRL (n = 9) subjects available from the study group. Data points represent DNA methylation percentage at the *PTPRD*-associated DMR. Mean values \pm SD are also shown. ***p < 0.001 in a two-tailed Mann–Whitney U-test. (B) *PTPRD* mRNA expression was measured by qPCR in SVF from FDR (n = 9) and control (CTRL; n = 11) subjects. Data points represent AU from each individual subject. Mean values \pm SD are also shown. **p < 0.01 in a two-tailed Mann–Whitney U-test. (C) Correlation between *PTPRD* DNA methylation and *PTPRD* mRNA levels in SVF from FDR (n = 8) and CTRL (n = 9) subjects. r correlation coefficient and p values are indicated on the graph. AU: Absolute units; BS: Bisulphite sequencing; CTRL: Control; DMR: Differentially methylated region; FDR: First-degree relatives; SD: Standard deviation; SVF: Stromal vascular fraction cells.

PTPRD epigenetic signature in peripheral blood leukocytes

Blood cells can be more easily accessed than the adipose tissue. Thus, search for epigenetic marks associated to disease traits has been so far largely conducted in blood [32]. Accordingly, we have further investigated whether the *PTPRD* hypomethylation observed in the SVF cells obtained from FDR individuals is accompanied by similar changes also in peripheral blood leukocytes.

Upon bisulphite treatment, we have sequenced the *PTPRD*-associated DMR in PBL from the same FDR and control subjects whose SVF cells have been previously assessed. Interestingly, similar as with the SVF cells, PBL methylation levels at *PTPRD* were also significantly decreased in the FDR subjects (Figure 6A). PBL DNA methylation at this locus also inversely correlated with subcutaneous adipose cell size (Figure 6B) in the study group. In addition, a positive correlation was established between *PTPRD* DNA methylation levels in PBL and SVF cells from each individual subject (Figure 6C), indicating that PBL represent a convenient proxy of the SVF epigenetic signature at this gene.

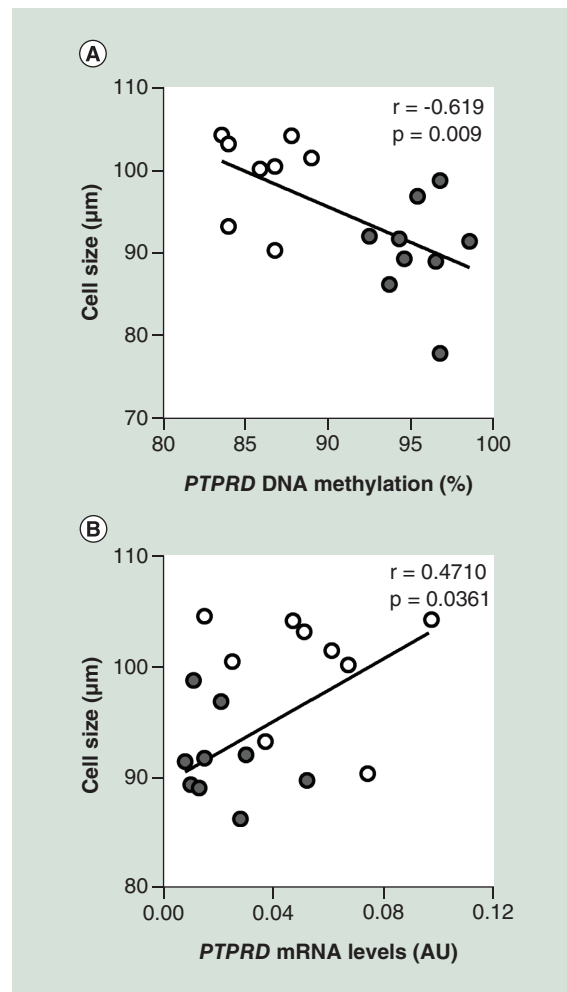


Figure 3. Correlation between subcutaneous adipose cell size, *PTPRD* DNA methylation and its mRNA levels. (A) Correlation between SVF *PTPRD* DNA methylation and adipose cell size in FDR (n = 8) and CTRL (n = 9) subjects. (B) Correlation between SVF *PTPRD* mRNA levels and adipose cell size in FDR (n = 9) and CTRL (n = 11) subjects. r correlation coefficient and p values are indicated on the graph. AU: Absolute units; CTRL: Control; FDR: First-degree relatives; SVF: Stromal vascular fraction cells.

Replication of the association to increased risk of T2D for the *PTPRD* DMR

Obesity, estimated by BMI, is one of the well-established risk factors for T2D [33]. Therefore, we sought to replicate the hypomethylation signal at the *PTPRD* gene in the PBL from an independent cohort of obese subjects. Similar to FDR, obese subjects have been reported to feature a higher risk of developing T2D (Supplementary Table 1). Interestingly, as evidenced in the FDR subjects, we observed that the PBL DNA methylation levels at *PTPRD* DMR were also significantly decreased in the obese compared with the lean individuals (Figure 7A). Of note, the *PTPRD* DNA methylation levels in PBL were found to negatively correlate with the BMI in these subjects (Figure 7B).

Discussion

In the present manuscript, we report the first genome-wide DNA methylation profile in human pre-adipocytes from healthy nonobese FDR. As previously described [4], these subjects are characterized by an ‘obese’ phenotype in the SAT even if they are normal weight, leading to a reduced insulin sensitivity and a more proatherogenic lipid profile with an increased risk of developing T2D. We found that, in SAT pre-adipocytes from the FDR individuals, a number of hypomethylation events associate to their *Methylome* profile and family history of T2D. Consistent with these novel findings and the high risk of T2D in FDR, T2D is also accompanied by whole genome hypomethylation events occurring both in the liver and in pancreatic islets [34,35]. Crujeiras and co-workers [36] have further reported the presence of hypomethylation in SAT and PBL genome from obese patients, who also feature excess risk of T2D [14]. Thus, the occurrence of hypomethylation events at specific genomic site in tissues representing major determinants of glucose homeostasis might contribute to increasing T2D risk. Indeed, our results in SAT from FDR are consistent with a previous study showing that the majority of the methylation changes associated with a family history of T2D in human skeletal muscle are hypomethylation events [37].

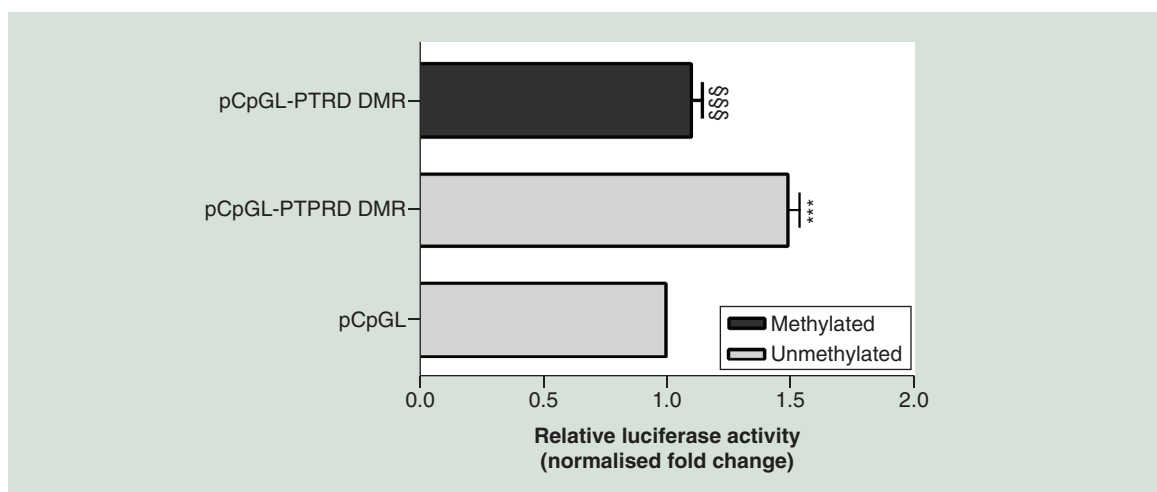


Figure 4. Effect of DNA methylation on *PTPRD* transcriptional activity. The 590 bp sequence corresponding to the intronic *PTPRD*-associated DMR *chr9:10448607-10450000*, was cloned into a pCpGL-promoter vector (pCpGL-*PTPRD* DMR), upstream the luciferase gene. The construct was either methylated by *M.SssI* (methylated pCpGL-*PTPRD* DMR) or mock-treated (unmethylated pCpGL-*PTPRD* DMR) and then transfected in Chub57 cells. The data were normalized using a co-transfected renilla luciferase vector and are presented as fold change relative to the mock-treated empty vector (pCpGL). Data are shown as means \pm SD of $n =$ three independent experiments. Statistical significance was tested by one-way ANOVA followed by Tukey's multi-comparison test: *** $p < 0.001$ for comparison versus pCpGL; §§§ $p < 0.001$ for comparison versus unmethylated pCpGL-*PTPRD* DMR. ANOVA: Analysis of variance; DMR: Differentially methylated region; SD: Standard deviation.

DNA methylation profiles are shaped by *DNMTs* [16]. In the present study, we report that the hypomethylation occurring at several genomic *loci* in the pre-adipocytes from FDR is accompanied by DNMT3A mRNA and protein downregulation, suggesting a causal relationship with at least some of the identified hypomethylation events. Indeed, previous studies document that DNMT3A inactivation decreases methylation at the genome-wide level in both human and mouse embryonic stem cells [38,39]. Evidence has also been reported that DNMT3A deficiency restricts adipogenesis [40,41]. We now find that the reduced expression of *DNMT3A* negatively correlates with SAT adipose cell hypertrophy in FDR, where the increased adipose cell size is a marker of impaired adipogenesis [2]. It is possible therefore that the downregulation of DNMT3A occurring in these subjects impacts on the methylation of distinct genomic regions which are relevant to adipogenesis, contributing to impair this function.

Functional analysis of the differential methylation profile identified in FDR led us to recognize that most DMG are related to biological pathways which are relevant to adipocyte biology or adipogenesis and T2D pathogenesis. These include the *Insulin* and *IGF*, *PKA*, *FGF* and *WNT* signalling cascades. Interestingly, methylation changes were more prevalent in gene body and intragenic regions as compared with gene promoter regions. This finding is consistent with previous studies by our own as well as other groups of investigators showing that DNA methylation events often involve regions other than promoters [15,42,43]. How gene body methylation may affect gene expression remains unclear [44–46]. However, our *Methylome* and *Transcriptome* findings in human FDR pre-adipocytes suggest that hypomethylation occurring at the gene body level may enhance gene expression; indeed, some genes in which both DNA methylation and mRNA expression were found simultaneously altered in the FDR pre-adipocytes show reduced methylation and increased expression.

In this study, *PTPRD* has been identified as the most significantly hypomethylated gene in FDR individuals. *PTPRD* encodes a transmembrane PTP termed *PTP δ* , which is highly homologous to the LAR protein and PTP σ tyrosine phosphatases [47]. All of them have been previously shown to modulate insulin signalling and may affect glucose tolerance *in vivo* [48–50]. Moreover, overexpression of LAR leads to suppression of adipocyte differentiation in both 3T3-L1 pre-adipocytes and human mesenchymal stem cells [51]. Whether these phosphatases also play a role in the evolution toward T2D and how, at the mechanistic level, these deranging functions occur has not yet been identified. Previous GWAS for T2D in a Han Chinese population have identified *PTPRD* as a T2D susceptibility gene [31]. Thus, the functional consequences of the *PTPRD* hypomethylation we have found in SVF from healthy FDR individuals deserve to be addressed. In this work, we have firstly shown that, in the

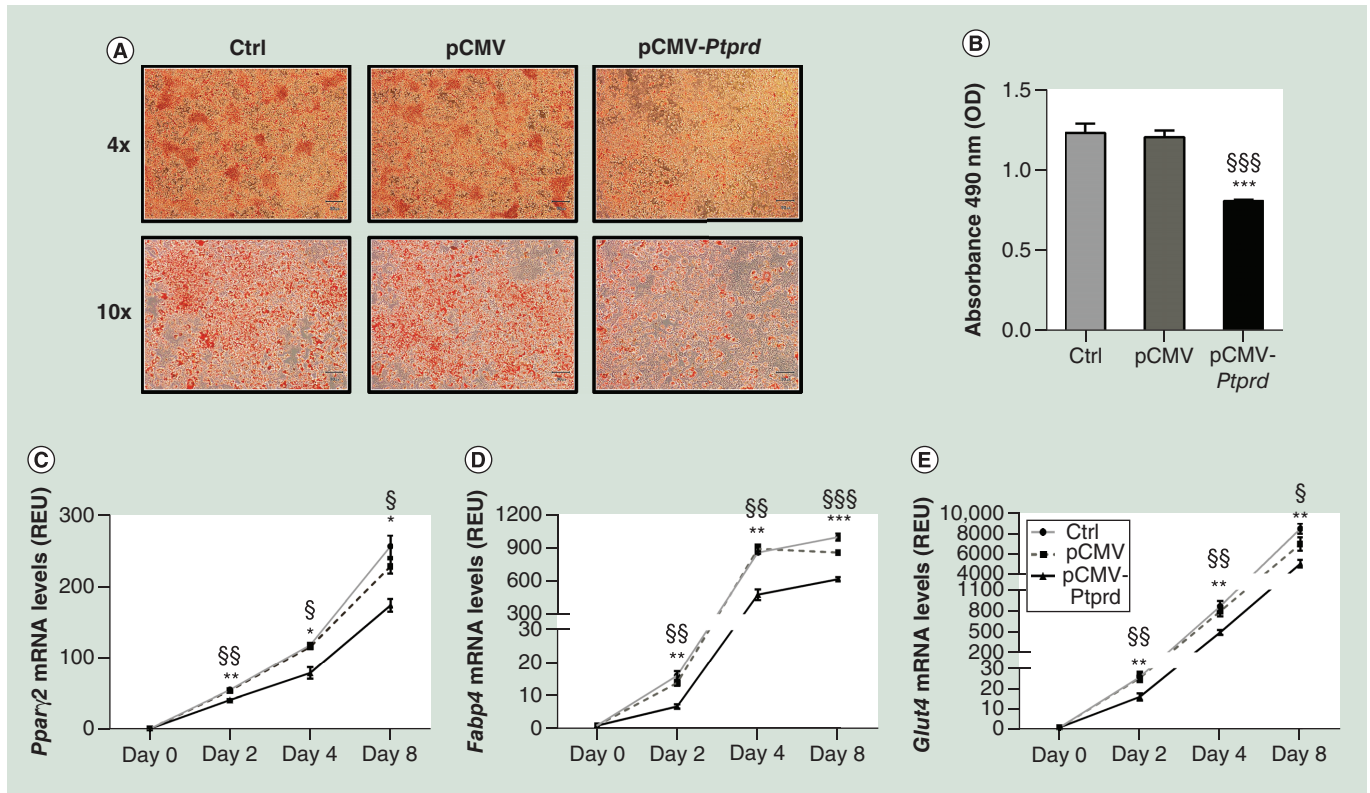


Figure 5. Effect of *PTPRD* overexpression on differentiation of 3T3-L1 pre-adipocytes. Un-transfected cells (Ctrl) and cells transfected with either the empty vector (pCMV) or the *PTPRD* expressing vector (pCMV-*PTPRD*), at differentiation day eight, were stained with Oil Red O and then subjected to phase contrast microscopy. Representative fields are shown in figure A. Lipid quantification (B) was assessed at 490 nm as described under Materials and methods. Expression levels of *Pparγ2* (C), *Fabp4* (D), and *Glut4* (E) were assessed by qPCR at the indicated time points. All data are presented as means \pm SD of $n = 3$ independent experiments. Statistical significance was tested by one-way ANOVA followed by Tukey's multi-comparison test at each indicated time point: * $p < 0.05$, ** $p < 0.01$, *** $p < 0.001$ for comparison versus Ctrl cells; § $p < 0.05$, §§ $p < 0.01$, §§§ $p < 0.001$ for comparison versus pCMV transfected cells. ANOVA: Analysis of variance; Ctrl: Control; OD: Optical density; pCMV: Cytomegalovirus promoter; REU: Relative expression units; SD: Standard deviation.

FDR pre-adipocytes, decreased methylation at the *PTPRD*-associated intronic DMR *chr9:10448607-10450000* is accompanied by *PTPRD* upregulation. Importantly, we demonstrated that methylation at this *locus* directly represses transcriptional activity of *PTPRD* *in vitro*, which may occur *in vivo* as well. This novel finding prompted us to hypothesize that methylation changes causing *PTPRD* upregulation contribute to the abnormalities in SAT function occurring in FDR and to the consequences of these abnormalities. Consistent with this hypothesis, we have found that methylation at the *PTPRD*-DMR negatively correlates with subcutaneous adipose cell size, while the *PTPRD* mRNA levels were positively correlated. In addition, we have further demonstrated that overexpression of *Ptprd* in cultured 3T3-L1 pre-adipocytes impairs their differentiation into mature adipocytes, as shown by reduced adipogenic gene expression and decreased lipid droplet accumulation. Collectively, these data suggest that, by impairing adipocyte precursor cell differentiation, methylation changes at *PTPRD* gene associate to increased risk of T2D in FDR.

The *PTPRD* methylation profile distinguishing SVF cells from FDR and from individuals who have no familiarity for T2D closely reflects that in blood-borne DNA obtained from PBL of the same study group subjects. Similar to the SVF adipocyte precursor cells, PBL methylation at the *PTPRD* *locus* negatively correlated with the subcutaneous adipose cell size in FDR where adipocyte hypertrophy is an independent predictor of T2D [4,5]. Thus, PBL seem to represent a convenient and easily accessible proxy of the SVF epigenetic profile at this gene in FDR. Our study further suggests the potential use of the *PTPRD* DNA methylation pattern in PBL as a promising biomarker of T2D risk since we have been able to replicate the FDR-associated *PTPRD* epigenetic profile in an independent cohort of severely obese patients, who feature – similar to the FDR individuals – an increased risk of T2D [33,52].

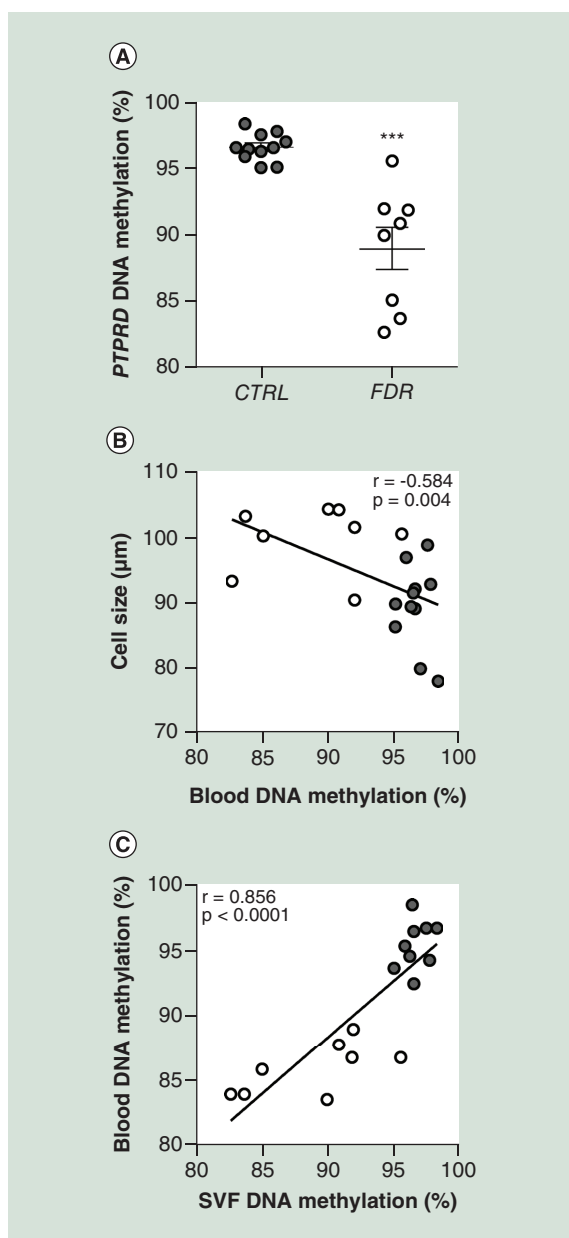


Figure 6. *PTPRD* DNA methylation in peripheral blood leukocytes from first-degree relative and CTRL subjects. (A) BS analysis of *PTPRD* DMR in PBL from FDR (n = 8) and CTRL (n = 11) subjects available from the study group. Data points represent DNA methylation percentage at the *PTPRD*-associated DMR. Mean values \pm SD are also shown. ***p < 0.001 in a two-tailed Mann–Whitney U-test. Correlation between PBL *PTPRD* DNA methylation and adipose cell size in FDR (n = 8) and CTRL (n = 11) (B) or SVF *PTPRD*. DNA methylation in FDR (n = 8) and CTRL (n = 9) subjects (C). *r* correlation coefficient and *p* values are indicated on the graph. BS: Bisulphite sequencing; CTRL: Control; DMR: Differentially methylated region; FDR: First-degree relatives; PBL: Peripheral blood leukocytes; SD: Standard deviation; SVF: Stromal vascular fraction cells.

Of note, the risk of T2D increases as BMI increases, from three-times in overweight people to more than 15-times in severely obese patients compared with individuals with a healthy BMI [53]. In our study, PBL DNA methylation at the *PTPRD* locus negatively correlated with BMI in individuals with severe obesity, strongly supporting a role for *PTPRD* methylation pattern in identifying individuals at high risk of developing T2D.

Previous investigations have shown that hypermethylation occurs at the *PTPRD* locus in PBL from Han Chinese individuals diagnosed to have T2D [54]. Interestingly, these methylation events were reported to induce down-regulation of *PTPRD* with progressive repression of its transcription with increasing duration of diabetes in the patients. These methylation changes may therefore be secondary to diabetes itself unlike those occurring in our FDR subjects who were not diabetic at the time they were recruited in the study. Importantly, these methylation events were caused by increased expression of *DNMT1*, which does not occur in our population, and involved the promoter rather than the intronic *chr9:10448607-10450000* region at *PTPRD*. The genetic background of the Han Chinese population and the subjects in our study group is likely different as *PTPRD* and *DNMT1* diabetes risk polymorphisms occurring in the former were not detected in the individuals we have studied (data not shown). This diversity might have contributed to the occurrence of different epigenetic profile in the two groups.

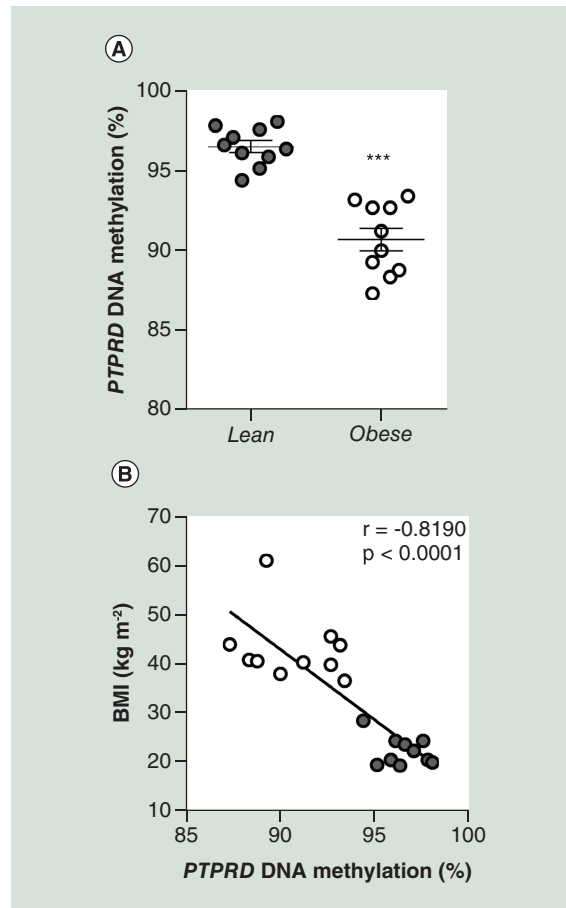


Figure 7. *PTPRD* DNA methylation in peripheral blood leukocytes from obese and lean subjects. (A) BS analysis of *PTPRD* DMR in PBL from obese ($n = 10$) and lean ($n = 10$) subjects from the replication group. Data points represent DNA methylation percentage at the *PTPRD*-associated DMR. Mean values \pm SD are also shown. *** $p < 0.001$ in a two-tailed Mann–Whitney U-test. **(B)** Correlation between PBL *PTPRD* DNA methylation and BMI in obese ($n = 10$) and lean ($n = 10$) subjects. r correlation coefficient and p values are indicated on the graph. BS: Bisulphite sequencing; DMR: Differentially methylated region; PBL: Peripheral blood leukocytes; SD: Standard deviation.

Although we have included two independent cohorts in our analyses and different types of tissues (i.e., PBL and SVF samples), we are aware that the small sample size of the recruited individuals could represent a limitation of our study which, however, deserves to be replicated in larger populations and analysed in further prospective studies.

Conclusion

This work provides the first genome-wide DNA methylation analysis in human adipocyte precursor cells from SAT of healthy non-obese individuals who are FDR of diabetic patients. It is shown that the *Methylome* profile of these subjects features significant differences at genes known to be implicated in both adipose cell function and T2D development. In addition, these studies have revealed a previously unrecognized function of *PTPRD* in restraining adipogenesis and found evidence that *PTPRD* hypomethylation, which is also reflected in blood-borne DNA, may contribute to adipose cell hypertrophy in FDR of T2D patients.

Future perspective

Use of data from the present work may, in the future, reveal epigenetic changes contributing to T2D risk. Some of these changes may further represent marks of disease applicable to prediction and treatment, particularly lifestyle-based treatment.

Supplementary data

To view the supplementary data that accompany this paper please visit the journal website at: www.futuremedicine.com/doi/suppl/10.2217/epi-2019-0267

Acknowledgments

The authors thank M Ceccarelli for his valuable support and comments.

Financial & competing interest disclosure

L Parrillo is the recipient of the SID-FO.DI.RI/MSD ITALIA 2017 Research Fellowship and the EFSD/Lilly Research Fellowship 2015. This study was funded, in part, by the European Foundation for the Study of Diabetes (EFSD), by the Ministero dell'Istruzione, Università e della Ricerca Scientifica, by Regione Campania POR FESR 2014–2020 (Obiettivo specific 1.2.) Manifestazione di Interesse per la Realizzazione di Technology Platform nell'ambito della Lotta alle Patologie Oncologiche" Projects: RARE PLAT NET, SATIN, and COEPICA, by the Società Italiana di Diabetologia (SID-FO.DI.RI), by the Swedish Research Council, Torsten Söderberg and by the Novo Nordisk Foundation. The authors have no other relevant affiliations or financial involvement with any organization or entity with a financial interest in or financial conflict with the subject matter or materials discussed in the manuscript apart from those disclosed.

No writing assistance was utilized in the production of this manuscript.

Ethical conduct of research

The authors state that they have obtained appropriate institutional review board approval for all human experimental investigations. In addition, for investigations involving human subjects, informed consent has been obtained from the participants involved.

Open access

This work is licensed under the Attribution-NonCommercial-NoDerivatives 4.0 Unported License. To view a copy of this license, visit <http://creativecommons.org/licenses/by-nc-nd/4.0/>

Summary points

- Epigenetic signature of first-degree relatives (FDR) subcutaneous adipose tissue (SAT) pre-adipocytes is characterized by global DNA hypomethylation.
- DNA methylation changes in FDR SAT pre-adipocytes occur in key genes implicated in adipocyte functions and Type 2 Diabetes.
- Hypomethylation at the *PTPRD* risk gene strongly associates with SAT hypertrophy in FDR subjects.
- Adipogenesis is impaired by *Ptprd* overexpression in cultured 3T3-L1 pre-adipocytes.
- Pre-adipocyte *PTPRD* hypomethylation reflects in blood-borne DNA, indicating that peripheral blood leukocytes represent a proxy of epigenetic signature at this locus.
- *PTPRD* hypomethylation could identify individuals with a high risk of developing Type 2 Diabetes.

References

Papers of special note have been highlighted as: ● of interest; ●● of considerable interest

1. Lönn M, Mehlige K, Bengtsson C, Lissner L. Adipocyte size predicts incidence of Type 2 diabetes in women. *FASEB J.* 24, 326–331 (2010).
2. Longo M, Raciti GA, Zatterale F *et al.* Epigenetic modifications of the *Zfp/ZNF423* gene control murine adipogenic commitment and are dysregulated in human hypertrophic obesity. *Diabetologia* 61, 369–380 (2018).
 - **Highlights the important role of DNA methylation in the functional regulation of genes determining adipogenesis.**
3. Longo M, Zatterale F, Naderi J *et al.* Adipose tissue dysfunction as determinant of obesity-associated metabolic complications. *Int. J. Mol. Sci.* 20(9), 2358 (2019).
4. Arner P, Arner E, Hammarstedt A, Smith U. Genetic predisposition for Type 2 diabetes, but not for overweight/obesity, is associated with a restricted adipogenesis. *PLoS ONE* 6, e18284 (2011).
 - **The first study regarding reduced subcutaneous adipogenesis as signature of family history for Type 2 Diabetes.**
5. InterAct Consortium, Scott RA, Langenberg C *et al.* The link between family history and risk of Type 2 diabetes is not explained by anthropometric, lifestyle or genetic risk factors: the EPIC-InterAct study. *Diabetologia* 56, 60–69 (2013).
6. Henninger AM, Eliasson B, Jenndahl LE, Hammarstedt A. Adipocyte hypertrophy, inflammation and fibrosis characterize subcutaneous adipose tissue of healthy, non-obese subjects predisposed to Type 2 diabetes. *PLoS ONE* 9, e105262 (2014).
7. Lotta LA, Gulati P, Day FR *et al.* Integrative genomic analysis implicates limited peripheral adipose storage capacity in the pathogenesis of human insulin resistance. *Nat. Genet.* 49, 17–26 (2014).
8. Cederberg H, Stančáková A, Kuusisto J, Laakso M, Smith U. Family history of Type 2 diabetes increases the risk of both obesity and its complications: is Type 2 diabetes a disease of inappropriate lipid storage? *J. Intern. Med.* 277, 540–551 (2015).
9. Smith U, Kahn BB. Adipose tissue regulates insulin sensitivity: role of adipogenesis, *de novo* lipogenesis and novel lipids. *J. Intern. Med.* 280, 465–475 (2016).

10. Acosta JR, Douagi I, Andersson DP *et al.* Increased fat cell size: a major phenotype of subcutaneous white adipose tissue in non-obese individuals with Type 2 diabetes. *Diabetologia* 59, 560–570 (2016).
11. Multhaup ML, Seldin MM, Jaffe AE *et al.* Mouse-human experimental epigenetic analysis unmasks dietary targets and genetic liability for diabetic phenotypes. *Cell Metab.* 21, 138–149 (2015).
12. Keller M, Hopp L, Liu X *et al.* Genome-wide DNA promoter methylation and transcriptome analysis in human adipose tissue unravels novel candidate genes for obesity. *Mol. Metab* 6, 86–100 (2016).
13. Rönn T, Volkov P, Davegårdh C *et al.* A six months exercise intervention influences the genome-wide DNA methylation pattern in human adipose tissue. *PLoS Genet.* 9, e1003572 (2013).
14. Vazquez G, Duval S, Jacobs DR Jr, Silventoinen K. Comparison of body mass index, waist circumference, and waist/hip ratio in predicting incident diabetes: a meta-analysis. *Epidemiol. Rev.* 29, 115–128 (2007).
15. Broholm C, Olsson AH, Perflyev A *et al.* Human adipogenesis is associated with genome-wide DNA methylation and gene-expression changes. *Epigenomics* 8, 1601–1617 (2016).
16. Parrillo L, Spinelli R, Nicolò A *et al.* Nutritional factors, DNA methylation, and risk of Type 2 diabetes and obesity: perspectives and challenges. *Int. J. Mol. Sci.* 20(12), 2983 (2019).
17. Parrillo L, Costa V, Raciti GA *et al.* Hoxa5 undergoes dynamic DNA methylation and transcriptional repression in the adipose tissue of mice exposed to high-fat diet. *Int. J. Obes. (Lond)* 40, 929–937 (2016).
- **Demonstrates that MeDIP-Seq represents an effective approach for DNA methylome analysis.**
18. Laakso M, Zilinskaite J, Hansen T *et al.* Insulin sensitivity, insulin release and glucagon-like peptide-1 levels in persons with impaired fasting glucose and/or impaired glucose tolerance in the EUGENE2 study. *Diabetologia* 51, 502–511 (2008).
19. Isakson P, Hammarstedt A, Gustafson B, Smith U. Impaired preadipocyte differentiation in human abdominal obesity: role of Wnt, tumor necrosis factor-alpha, and inflammation. *Diabetes* 58, 1550–1557 (2009).
20. Desiderio A, Longo M, Parrillo L *et al.* Epigenetic silencing of the ANKRD26 gene correlates to the pro-inflammatory profile and increased cardio-metabolic risk factors in human obesity. *Clin. Epigenetics* 11, 181 (2019).
21. Li H, Handsaker B, Wysoker A *et al.* The Sequence Alignment/Map format and SAMtools. *Bioinformatics* 25, 2078–2079 (2009).
22. Zhang Y, Liu T, Meyer CA *et al.* Model-based analysis of ChIP-Seq (MACS). *Genome Biol.* 9, R137 (2008).
23. Robinson MD, McCarthy DJ, Smyth GK. edgeR: a Bioconductor package for differential expression analysis of digital gene expression data. *Bioinformatics* 26, 139–140 (2010).
24. Benjamini Y, Hochberg Y. Controlling the false discovery rate – a practical and powerful approach to multiple testing. *J. Royal Statist. Soc., Series B.* 57, 289–300 (1995).
25. Li B, Dewey CN. RSEM: accurate transcript quantification from RNA-Seq data with or without a reference genome. *BMC Bioinformatics* 12, 323 (2011).
26. de Cristofaro T, Di Palma T, Fichera I *et al.* An essential role for Pax8 in the transcriptional regulation of cadherin-16 in thyroid cells. *Mol. Endocrinol.* 26, 67–78 (2012).
27. Raciti GA, Spinelli R, Desiderio A *et al.* Specific CpG hyper-methylation leads to Ankrd26 gene down-regulation in white adipose tissue of a mouse model of diet-induced obesity. *Sci. Rep.* 7, 43526 (2017).
28. Liotti A, Cabaro S, Cimmino I *et al.* Prep1 deficiency improves metabolic response in white adipose tissue. *Biochim. Biophys. Acta* 1863(5), 515–525 (2018).
29. Longo M, Spinelli R, D'Esposito V *et al.* Pathologic endoplasmic reticulum stress induced by glucotoxic insults inhibits adipocyte differentiation and induces an inflammatory phenotype. *Biochim. Biophys. Acta* 1863, 1146–1156 (2016).
30. Lyko F. The DNA methyltransferase family: a versatile toolkit for epigenetic regulation. *Nat. Rev. Genet.* 19, 81–92 (2018).
31. Tsai FJ, Yang CF, Chen CC *et al.* A genome-wide association study identifies susceptibility variants for Type 2 diabetes in Han Chinese. *PLoS Genet.* 6, e1000847 (2010).
- **Identifies *PTPRD* as a Type 2 Diabetes susceptibility locus via a large-scale genome-wide examination**
32. Barciszewska AM, Nowak S, Naskręć-Barciszewska MZ. The degree of global DNA hypomethylation in peripheral blood correlates with that in matched tumor tissues in several neoplasia. *PLoS ONE* 9, e92599 (2014).
- **Reports that DNA methylation measured in whole blood is a marker for other tissues directly involved in disease.**
33. Laakso M. Biomarkers for Type 2 diabetes. *Mol. Metab.* 27S, S139–S146 (2019).
34. Nilsson E, Matte A, Perflyev A *et al.* Epigenetic alterations in human liver from subjects with Type 2 diabetes in parallel with reduced folate levels. *J. Clin. Endocrinol. Metab.* 100, e1491–e1501 (2015).
35. Dayeh T, Volkov P, Salö S *et al.* Genome-wide DNA methylation analysis of human pancreatic islets from type 2 diabetic and nondiabetic donors identifies candidate genes that influence insulin secretion. *PLoS Genet.* 10(3), e1004160 (2014).
36. Crujeiras AB, Diaz-Lagares A, Sandoval J *et al.* DNA methylation map in circulating leukocytes mirrors subcutaneous adipose tissue methylation pattern: a genome-wide analysis from non-obese and obese patients. *Sci. Rep.* 7, 41903 (2017).

37. Nitert MD, Dayeh T, Volkov P *et al.* Impact of an exercise intervention on DNA methylation in skeletal muscle from first-degree relatives of patients with Type 2 diabetes. *Diabetes* 61, 3322–3332 (2012).
38. Chen T, Ueda Y, Dodge JE, Wang Z, Li E. Establishment and maintenance of genomic methylation patterns in mouse embryonic stem cells by Dnmt3a and Dnmt3b. *Mol. Cell. Biol.* 23, 5594–5605 (2003).
39. Liao J, Karnik R, Gu H *et al.* Targeted disruption of DNMT1, DNMT3A and DNMT3B in human embryonic stem cells. *Nat. Genet.* 47, 469–478 (2015).
40. Yang X, Wu R, Shan W, Yu L, Xue B, Shi H. DNA methylation biphasically regulates 3T3-L1 preadipocyte differentiation. *Mol. Endocrinol.* 30, 677–687 (2016).
41. Guo W, Chen J, Yang Y, Zhu J, Wu J. Epigenetic programming of Dnmt3a mediated by AP2 α is required for granting preadipocyte the ability to differentiate. *Cell Death Dis.* 7, e2496 (2016).
42. Zhang P, Zhao M, Liang G *et al.* Whole-genome DNA methylation in skin lesions from patients with psoriasis vulgaris. *J. Autoimmun.* 41, 17–24 (2013).
43. Maunakea AK, Nagarajan RP, Bilenky M *et al.* Conserved role of intragenic DNA methylation in regulating alternative promoters. *Nature* 466, 253–257 (2010).
44. Jones PA. Functions of DNA methylation: islands, start sites, gene bodies and beyond. *Nat. Rev. Genet.* 13, 484–492 (2012).
45. Blattler A, Yao L, Witt H *et al.* Global loss of DNA methylation uncovers intronic enhancers in genes showing expression changes. *Genome Biol.* 15, 469 (2014).
46. Bakshi A, Bretz CL, Cain TL, Kim J. Intergenic and intronic DNA hypomethylated regions as putative regulators of imprinted domains. *Epigenomics* 10, 445–461 (2018).
- **Underlines the significance of gene body methylation to transcriptional regulation.**
47. Toker AW. Protein tyrosine phosphatases and signalling. *J. Endocrinol.* 185, 19–33 (2005).
48. Ren JM, Li PM, Zhang WR *et al.* Transgenic mice deficient in the LAR protein-tyrosine phosphatase exhibit profound defects in glucose homeostasis. *Diabetes* 47, 493–497 (1998).
49. Chagnon MJ, Elchebly M, Uetani N *et al.* Altered glucose homeostasis in mice lacking the receptor protein tyrosine phosphatase sigma. *Can. J. Physiol. Pharmacol.* 84, 755–763 (2006).
50. Batt J, Asa S, Fladd C, Rotin D. Pituitary, pancreatic and gut neuroendocrine defects in protein tyrosine phosphatase-sigma-deficient mice. *Mol. Endocrinol.* 16, 155–169 (2002).
51. Kim WK, Jung H, Kim DH *et al.* Regulation of adipogenic differentiation by LAR tyrosine phosphatase in human mesenchymal stem cells and 3T3-L1 preadipocytes. *J. Cell Sci.* 122, 4160–4167 (2009).
52. Corbin LJ, Richmond RC, Wade KH *et al.* BMI as a modifiable risk factor for Type 2 Diabetes: refining and understanding causal estimates using mendelian randomization. *Diabetes* 65, 3002–3007 (2016).
53. Kivimäki M, Kuosma E, Ferrie JE *et al.* Overweight, obesity, and risk of cardiometabolic multimorbidity: pooled analysis of individual-level data for 120 813 adults from 16 cohort studies from the USA and Europe. *Lancet Public Health* 2, e277–e285 (2016).
54. Chen YT, Lin WD, Liao WL, Lin YJ, Chang JG, Tsai FJ. PTPRD silencing by DNA hypermethylation decreases insulin receptor signaling and leads to Type 2 diabetes. *Oncotarget* 6, 12997–13005 (2015).